Constitutive activation of mutant glycogen synthase in equine type 1 polysaccharide storage myopathy explains the gain of function disease mechanism in a highly prevalent model of cellular polyglucosan formation

Maile, C.A. [1], Hingst, J. R.[2], Mahalingan, K. K.[3], O'Reilly, A. O.[4], Cleasby, M. E.[5], Mickelson, J. R. [6], McCue, M. E. [7], Hurley, T. D.[3], Wojtaszewski, J. F. P.[2], Piercy, R. J. [1]

Comparative Neuromuscular Diseases Laboratory, Department of Clinical Sciences and Services[1] and Department of Comparative Biomedical Sciences[5], Royal Veterinary College, London, UK, The August Krogh Centre, Department of Nutrition, Exercise and Sports, University of Copenhagen, Denmark[2], Department of Biochemistry and Molecular Biology, Indiana University School of Medicine[3], School of Natural Sciences and Psychology, Liverpool John Moores University, Liverpool, UK.[4] Veterinary Biological Sciences Department[6] and Veterinary Population Medicine Department[7], University of Minnesota, 1365 Gortner Ave., St. Paul, MN, USA

Corresponding author: Professor Richard Piercy, Comparative Neuromuscular Diseases Laboratory, Department of Clinical Sciences and Services, The Royal Veterinary College, Royal College Street, London, NW1 0TU. UK. Tel: 0044 207 468 5000 Email: rpiercy@rvc.ac.uk

Summary

Equine type 1 polysaccharide storage myopathy (PSSM1) is associated with a missense, founder mutation (R309H) in the *GYS1* glycogen synthase gene, excessive glycogen and amylopectate-like inclusions in muscle, and higher muscle glycogen synthase (GS) activities than in controls; however, the causative mechanisms remain unclear. GS is allosterically regulated by glucose-6-phosphate (G6P) and enzyme activity is reduced by phosphorylation. In this work, homology modelling, and equine muscle biochemical and recombinant enzyme kinetic assays *in vitro* were used to investigate the hypothesis that higher GS activity in affected horses is due to (1) a conformational structural change; (2) higher expression of the mutant enzyme; (3) reduced phosphorylation or (4) constitutive activation.

PSSM1-affected horses had significantly higher muscle glycogen contents than controls. Despite no difference in total expression, GS activity was significantly higher in PSSM1-affected homozygotes than in heterozygotes and control horses in both the absence ($p=0.04$) and presence ($p=0.03$) of G6P. There was significantly more phosphorylation of GS at site 2+2a ($p=0.009$) and a significantly higher AMPK (an upstream kinase) expression ($p=0.04$) in PSSM1-homozygotes compared to controls. In contrast to recombinant wild type enzyme, mutant GS was highly active, even at very low G6P concentrations.

The mutant enzyme's high activity, despite increased phosphorylation, even in the absence of G6P, reveals it to be constitutively active. Modelling suggests that the R309H mutation disrupts a salt bridge that normally stabilises the enzyme's basal state, shifting the conformational equilibrium to the active state and explaining the gain-of-function pathogenesis in this highly prevalent disorder.

Key words: PSSM1, Glycogen synthase, glycogen, horse, glycogen storage disorder,

Introduction

The ability to store glucose as the branched chain polymer glycogen is shared by organisms as evolutionarily diverse as bacteria and mammals: it enables organisms to deal with temporary starvation by maintaining energy provision through glycogen catabolism, and, in times of plenty, to store this energy macromolecule substrate in a form that has minimal effect on cellular osmotic pressure [1]. In mammals, glycogen is normally stored in muscle and other tissues following the action of 2 enzymes: glycogen synthase (GS) and glycogen branching enzyme (GBE). GS catalyses the polymerisation of UDP-glucose monomers via α1-4 glycosidic bonds and GBE is responsible for generating α1-6 bonds, every 4-10 residues [2]. There are 2 GS isoforms; one, muscle glycogen synthase (MGS) is encoded by the *GYS1* gene and predominantly expressed in muscle but also in other tissues; the other, liver glycogen synthase (LGS) is encoded specifically in liver, a product of the *GYS2* gene. Both GS isoforms are regulated by phosphorylation and allosteric modulation by glucose-6-phosphate (G6P) [3].

There are more than 14 glycogen storage diseases in humans and animals [4-7], several of which are characterised by excessive glycogen accumulation or abnormal glycogen structure caused by defects in glycogenesis or glycogenolysis. In 2008, a missense, autosomal dominant mutation (R309H) in *GYS1* was identified in Quarter Horses with a form of exertional rhabdomyolysis known as polysaccharide storage myopathy (PSSM1), characterised by excessive glycogen and amylopectate accumulation in skeletal muscle [8] but without apparent cardiac signs [9]. Since then, the identical mutation has been reported in many horse breeds worldwide [10-13], suggesting dissemination from a single founder, and there is evidence supporting positive selection for the mutation within certain breeds [14] which might be associated with the mutation's effect on increasing enzyme activity [8]. Since the ratio of GS: GBE activity is important in formation of glycogen with a normal structure [15], filamentous alpha crystalline polysaccharide that forms in PSSM1-affected muscle likely develops due to an increased GS: GBE activity [16]. However, the mechanism by which the R309H mutation results in increased GS activity is unknown; potential mechanisms include elevated expression, reduced degradation or dysregulation of enzyme activity. Since mutation of an adjacent amino acid in the yeast GS

(equivalent to amino acid G310 in mammalian GS) also results in increased enzyme activity [17], mutations in this region might result in constitutive activation of the enzyme.

Aberrant phosphorylation of the mutant enzyme might account for the increase in GS activity seen in horses with PSSM1 [8]. GS regulation is heavily dependent on 9 separate phosphorylation sites that are modified by various upstream kinases; of these, phosphorylation at sites 2 (serine residue S7), 2a (S10), 3a (S641) and 3b (S645) decrease the enzyme's activity more than the remaining 5 sites [18-20]. Furthermore, phosphorylation of certain sites enables sequential phosphorylation of others so that they can be functionally grouped for investigative purposes [21]. The phosphorylation sites are arranged into clusters where a primary site must be phosphorylated prior to sequential phosphorylation of the other surrounding sites in a process known as hierarchical phosphorylation [21]. Two of the key upstream kinases for GS are glycogen synthase kinase 3β (GSK3β) (which phosphorylates sites 3a, 3b, 3c, and 3d) and AMP-activated protein kinase (AMPK), which phosphorylates site 2. The phosphorylation of these sites markedly inactivate GS, whereas other upstream regulators, namely Casein Kinase 2 and Protein kinase A, are associated with phosphorylation as sites 1a, 1b and 5 which have little effect on GS activity [21].

AMPK exists as a heterotrimer made up of an α□□catalytic□, a β (regulatory) and a γ (regulatory) subunit [23]. Both α1 and α2 forms are expressed in skeletal muscle but it is the α1 form that contributes mainly to AMPK activity at rest and the α2 form which increases in response to exercise, therefore suggesting the α1 form is the 'basal' form of the enzyme found in skeletal muscle [24]. The phosphorylation of GS can also have a significant effect on G6P affinity; indeed, regulation by G6P is associated with a feed-forward mechanism resulting in further enzyme activation by dephosphorylation [22]. Although the R309H residue is distant in the primary sequence from any of the known phosphorylation sites, the mutation could result in an inappropriate response to phosphorylation as is seen in a yeast GS variant [17]. Dranchak *et al.* examined activity of AMPK in horses with PSSM in comparison with controls (finding no difference) prior to identification of the equine *GYS1* mutation [25], but expression or

phosphorylation of other upstream regulators, such as GSK3β, have not been investigated in this disorder.

Although the crystal structure has not been published for any mammalian glycogen synthase, the structures for a bacterial GT5 synthase (*Agrobacterium tumefaciens*) [2] and, more recently, for a yeast synthase (*Saccharomyces cerevisiae*; Gsy2p) [26] and *Caenorhabditis elegans* [27] have been solved. Yeast GS is a homo-tetrameric protein in both its basal and active states and eukaryotic GT3 synthases likely have a similar tetrameric arrangement due to their high levels of sequence homology [26]. Since the amino acid sequence surrounding the PSSM1 R309H *GYS1* mutation is highly conserved amongst species, from yeast to horses [8] this site might have an important (but as yet unknown) functional role [2, 28], although it is not thought to be involved in substrate binding [2, 29] or catalytic activity [2, 17, 30].

The binding of the GS ligand, G6P is complex, given its dual roles as both an allosteric activator and substrate [26]. The structural basis for G6P allosteric activation has been revealed from analysis of high-resolution crystal structures of the homologous synthase enzyme, Gsy2p from *Saccharomyces cerevisiae*; GS has a binding pocket for the 6-phosphate side chain of G6P that comprises 5 residues that are conserved across the GT3 family glycosyltransferases [26]. Subsequently, G6P binding results in a major conformational change involving translation and rotation toward the tetramer interface of the enzyme to generate the active form [26]. Co-crystallisation of Gsy2p with maltodextrin polymers (used as analogues to detect glycogen binding sites) shows that there are at least 4 maltodextrin sites for this substrate in the enzyme's active form [31]. Only binding sites 1 and 2 are exposed in the basal form of GS [31]: these sites might be important for enabling the enzyme to remain bound to glycogen even when GS activity is reduced by phosphorylation [32].

Improved understanding of the mechanism by which a mutation in equine *GYS1* leads to the mutant enzyme's increased activity might help further elucidate the functional significance of a region of this fundamentally important mammalian enzyme. Furthermore, it might prompt

investigation of specific treatments for this common equine myopathy or for other related glycogenosis in humans [33]. In this work, we investigate the enzyme's regulation *in silico* via computational modelling and through biochemical analysis *in vitro* of whole muscle extracts and via insect-derived recombinant enzyme kinetics. We hypothesised that higher GS activity in PSSM1-affected horses might be due either to (1) a conformational change associated with ligand binding or to the active site; (2) increased expression or reduced degradation of the mutant enzyme, (3) reduced phosphorylation or (4) constitutive activation.

Materials and Methods

Muscle sample collection:

Muscle samples were collected by open biopsy under local anaesthesia from the semimembranosus muscle of 12 normal (RR), 13 heterozygote (HR) and 4 homozygous mutant (HH) Belgian Draught and Percheron horses according to ethical approval from the Institutional Animal Care and Use Committee (University of Auburn). All horses were maintained at the University research facility and were managed at pasture and fed identically. Horses were selected on the basis of age- and sex-matching of individuals of differing genotype; following genotyping of the entire herd of horses using an established restriction fragment polymorphism assay [8]. Samples were snap-frozen in liquid nitrogen, shipped on dry ice and stored at -80^{o}C until use.

Glycogen content measurement:

Total glycogen was measured in 50 mg wet weight muscle biopsy samples using a commonly used colorimetric assay [34] (RR=6, RH=6, HH=4).

GS activity:

GS activity was measured using radiolabelled glucose [35] in the presence of low (0.02 mM), medium (0.17 mM) and high (8 mM) G6P concentrations; this enables the calculation of fractional velocity of the enzyme, %FV (comparison of medium to high G6P activities) and G6P-independent activity, I-form (comparison of low to high G6P values)[35]. These calculations enable

investigation of the regulation of GS by G6P (%FV) and by phosphorylation (independent of G6P concentrations) (I-form) [35-37]. Briefly, 20 µg of homogenised muscle (RR n=12, RH n=13, HH n=4) was placed into wells of a 96 well plate (Nunc) in duplicate and 40 µl of each of 3 different glucose concentration reagents was added (final glucose concentrations of 0.02 mM, 0.17 mM or 8 mM). Samples were incubated with the glucose reagent for 25 minutes at 37 ^{o}C and then 50 µl of the mixture was added to wells of Unifilter 96 well plates (Whatman) containing 200 µl 66% ice-cold ethanol in ddH_20 water. The plates were then incubated at -20 ^{o}C for 2 h and subsequently washed in ice-cold 66% ethanol 5 times. Plates were then dried for 15 minutes at 37 ^{o}C and 75 µl of Microscint 40 scintillation fluid (Perkin Elmer) was added to each well before counting using a top-count NXT scintillation counter (Perkin Elmer).

Muscle homogenisation:

For total GS expression, homogenates were prepared from 50 mg of snap frozen muscle tissue dissected free of any visible fat or connective tissue and crushed using an ice-cold pestle and mortar. The powder was then dissolved in 1 ml of protein extraction buffer containing phosphatase inhibitors, heated at 100 ^{o}C for 5 minutes and subsequently centrifuged (16000g for 5 minutes at 4 ^{o}C). The supernatant was removed and its protein concentration measured using the Pierce BCA protein assay.

For phosphorylated isoforms of GS and upstream kinases, a modified extraction method was performed. 40 mg of frozen muscle was cut into small pieces and submerged in 600 ul of protein extraction buffer, before homogenising using a Qiagen TissueLyser (2 x 30 seconds at 30000 Hz). The samples were then rotated end over end for 1 h at 4 ^{o}C and protein concentration was subsequently determined as above.

Total glycogen synthase expression:

Whole muscle protein homogenates were separated using 8% acrylamide gels and transferred onto nitrocellulose membranes (Amersham). Total GS expression was measured using a rabbit monoclonal antibody to the C-terminus of human glycogen synthase (Clone EP817Y; Epitomics;

1: 10000) and membranes were co-blotted with a mouse monoclonal antibody to human desmin (Clone D33, Dako; 1: 50000). Secondary antibodies were HRP-conjugated goat antibodies (either anti-rabbit or anti-mouse; BioRad; 1:5000). All antibodies were incubated for 1 hour at room temperature. Chemiluminescence was measured with the ECL-prime kit (Amersham) and Amersham Hyperfilm ECL (GE Healthcare). Assay linearity was confirmed through pilot experiments via loading of increasing amounts of protein per lane (results not shown). Films were digitised using a Stylus Photo RX640 printer and scanner (Epson, Hemel Hempstead, UK) alongside a 21-step transmission step wedge (Stouffer Graphic Arts, Mishawaka, USA). The mean grey intensity values from equal rectangular areas of each region of the step wedge were quantified in ImageJ (NIH, Bethesda, USA). Total GS expression was calculated as a ratio to desmin expression to control for loading.

Phosphorylated GS isoform expression:

Muscle protein samples were separated using 8% acrylamide gels and then transferred using a semi-dry technique (Amersham TE77) onto a PVDF membrane (Millipore). Sheep polyclonal primary antibodies were those used previously against phosphorylation epitopes of sites 1b (2 µg/ml), 2+2a (4 µg/ml) and 3a+b (1 µg/ml) of GS [35, 38]. The relevant HRP-conjugated secondary antibodies were used (Dako; 1:5000). All antibodies were incubated for 1 hour at room temperature. Chemiluminesence was measured using Luminata Forte HRP chemiluminescent subrstrate (Millipore). After quantification using ImageLab software (Biorad), membranes were stripped of antibodies and then re-incubated with a total GS antibody as previously described to normalise the data. Results are presented as a ratio to total GS expression.

GLUT4, GSK3□ and AMPK phosphorylation and expression:

Using the same technique as per phosphorylated isoforms of GS, total GLUT4 (Pierce; 1:1000), total GSK3β□□□D transduction Laboratories; 1:500) and AMPK (α1; 1:5000, α2; 1:15000 and β1; 1:1000, as described by Woods et al. [39]; β2:1:3000 as described by Durante et al. [40] and pAMPK Thr172; 1:1000 from Cell Signalling) expression levels were measured in whole muscle protein homogenates. Antibodies directed at the γ1 and γ3 subunits did not detect the equine

protein. All primary antibodies were diluted in 2% skimmed milk and incubated overnight at 4 ^{o}C and all secondary antibodies were incubated for 45minutes at room temperature. The relevant HRP-conjugated secondary antibodies were used (Dako; 1:5000). GLUT4 and GSK3β expression was quantified in muscle protein samples using α-actin (Sigma; 1:8000) as a loading control. AMPK expression was calculated and normalised according to a standard curve derived from protein homogenates of known quantities as is custom for this assay [41]. Chemiluminesence was measured using Luminata Forte HRP chemiluminescent substrate (Millipore) and quantified using ImageLab software (BioRad).

Statistical analysis:

Data calculations and statistical analysis were performed using GraphPad Prism (Version 6.0). Due to the small sample size for the homozygous mutant group, non-parametric statistics were performed and statistical significance was assessed via a Kruskal-Wallis test and Dunn's post-hoc multiple comparison test. Results were considered statistically significant when $P<0.05$. Pearson's correlation was used to examine association between continuous variables.

Homology modelling

X-ray crystal structures of *S. cerevisiae* Gsy2p in the basal state (PDB code 3NAZ; 3 Å resolution) and G6P-bound state (PDB code 3NB0; 2.41 Å resolution) provided the templates for homology modelling of equine GS. The full-length sequence of equine GS was retrieved from Genbank (accession ACB14276) and sequence aligned with *S. cerevisiae* Gsy2p using Clustal Omega [42]. MODELLER software [43] was used to generate 50 models of both the basal and bound tetrameric forms of equine GS. In both cases the internal scoring function of MODELLER was used to select 10 models that were visually inspected and submitted to the VADAR webserver [44] for assessment of stereochemical soundness in order to select a single best model. The R309H mutation was introduced into both models using SwissPDBViewer [45]. Model figures were generated using PyMOL (DeLano Scientific, San Carlos, CA, U.S.A.).

GS baculovirus cloning and expression

Wild-type GS and mutant R309H GS cDNAs were cloned into the PH promoter of the pFastBac dual vector (Invitrogen). Subsequently the equine glycogenin (GYG1) cDNA was subcloned into the p10 promoter of both the wild-type GS*pFastBac and the R309H mutant Gs*pFastbacs, allowing co-expression of the active form of equine GS with equine glycogenin in *Spodoptera frugiperda* Sf9 insect cells. Each of the cloned insert sequences in each vector was verified with Sanger sequencing. Western blot analysis of harvested insect cells from each of 3 different clones of mutant and wild type GS inserts was then used to confirm the expression of wild-type GS and R309H GS along with glycogenin. 1 litre culture of these cells were grown and cell pellets harvested by Kinnakeet Biotechnology

Purification of recombinant horse glycogen synthase

The insect cell pellet was resuspended and lysed in 50 mL of extraction buffer containing 50 mM Tris-HCl, pH 7.8, 300 mM NaCl, 0.1% Triton X-100, 2 mM ethylene-diamine-tetra-aceticacid (EDTA), 1 mM Benzamidine, 0.5 mM phenylmethanesulfonyl fluoride (PMSF), 10 mM β-mercaptoethanol (BME). The crude cell extract was centrifuged at 35,000 rpm in a Beckman Ti-45 rotor for 30 minutes at 4˚C and the supernatant was collected. To the clarified cell lysate, ethanol (kept at -80˚C prior to use) was slowly added under constant stirring to a final concentration of 30%. This process is done in an ice/salt broth so that the temperature stays between -1 and -5˚ C, ensuring complete precipitation of the endogenous insect cell glycogen (no additional glycogen was added). The suspension was then centrifuged at 9000g for 60 min at -3˚C. The supernatant was discarded and the glycogen pellet was resuspended in 100 ml of loading buffer containing 50 mM Tris-HCl, 300 mM NaCl, 1 mM Benzamidine, 0.5 mM PMSF and 2 mM BME. The resuspended pellet was then loaded onto a Concanavalin-A (Sigma) column. After washing the column with 20 column volumes of loading buffer, the protein was gradient eluted with glucose (0-400 mM). The fractions that had GS activity (in the presence of 10 mM G6P) was pooled and then dialyzed extensively against a buffer containing 50 mM Tris-HCl, 300 mM NaCl and 2 mM BME to remove the free glucose. The protein was then concentrated and mixed with glycerol to a final concentration of 35% and stored at -20˚ C for long term usage [46].

Specific activity and activity ratio measurement

Glycogen synthase activity was measured in the recombinant enzymes by the method of Thomas *et al*. which quantifies the amount of ^{14}C-glucose transferred from ^{14}C-labelled UDP-Glucose to glycogen over a period of 15 min at 30˚C [47]. Standard reaction conditions used 4.44 mM UDP-Glucose and 6.67 mg/ml of glycogen. Activity was measured both in the presence or absence of 10 mM G6P. The activity ratio is the ratio of the activity in the absence of G6P to the activity in the presence of 10 mM G6P. Protein concentration was measured by Bradford's method, using bovine serum albumin as a standard. Prior to use, rabbit liver glycogen type-III was deionized by passing it through TMD-8 hydrogen and hydroxide form mixed bed exchanger resins.

Enzyme Kinetics for UDP-Glucose and Glucose-6-Phosphate

For the UDP-Glucose (UDPG) titrations, 7 different concentrations of UDPG (0.1 mM to 15 mM for the WT enzyme and 0.05 mM to 6 mM for the mutant R309H enzyme) were used keeping the glycogen concentration constant at 6.67 mg/ml either in the presence or absence of 10 mM G6P. Eight different concentrations of G6P were used for the G6P titrations under standard reaction conditions.

Kinetic data analysis

The enzyme kinetic data were analyzed with using SigmaPlot (v12.3). The activation curves for G6P were fitted to the 4 parameter logistic curve and the $S_{0.5}$ values were obtained from these fits. The substrate saturation curves were fitted to the standard Michaelis-Menten equation $v= V_{max}*[S]/(K_m+[S])$, where v is the reaction rate, [S] is the substrate concentration, V_{max} is the maximum rate achieved by the system and K_m is the substrate concentration at half maximum velocity. The V_{max} and K_m values were obtained from these fits and the results represent the mean of 3 separate experiments.

Results

Breed and signalment data

There was no difference in age, sex or breed of the three genotyped groups used for this study. Signalment data is provided in table S1.

Glycogen content, GS activity and total GS expression.

Horses with the R309H mutation (heterozygote (RH) and homozygote (HH)) had significantly higher glycogen content in skeletal muscle than control (RR) horses (Figure 1A), although there was no difference between glycogen content in muscle from PSSM1-homozygote and PSSM1-heterozygote horses. The higher glycogen content of mutant horse muscle was accompanied by higher GS activity in muscle samples from homozygotes (HH) compared to samples from heterozygotes and between homozygotes (HH) and WT controls (RR) in the absence (0.02 mM G6P) and presence (0.02 mM) of G6P respectively ($p=0.04$, $p=0.03$) (Figure 1B and 1D) but there was no difference in total maximal GS activity between genotypes ($p=0.20$, data not shown). Thereby suggesting an increased sensitivity to regulation by G6P. There was no difference between total glycogen synthase protein expression in muscle samples in each of the genotyped groups (Figure 1C).

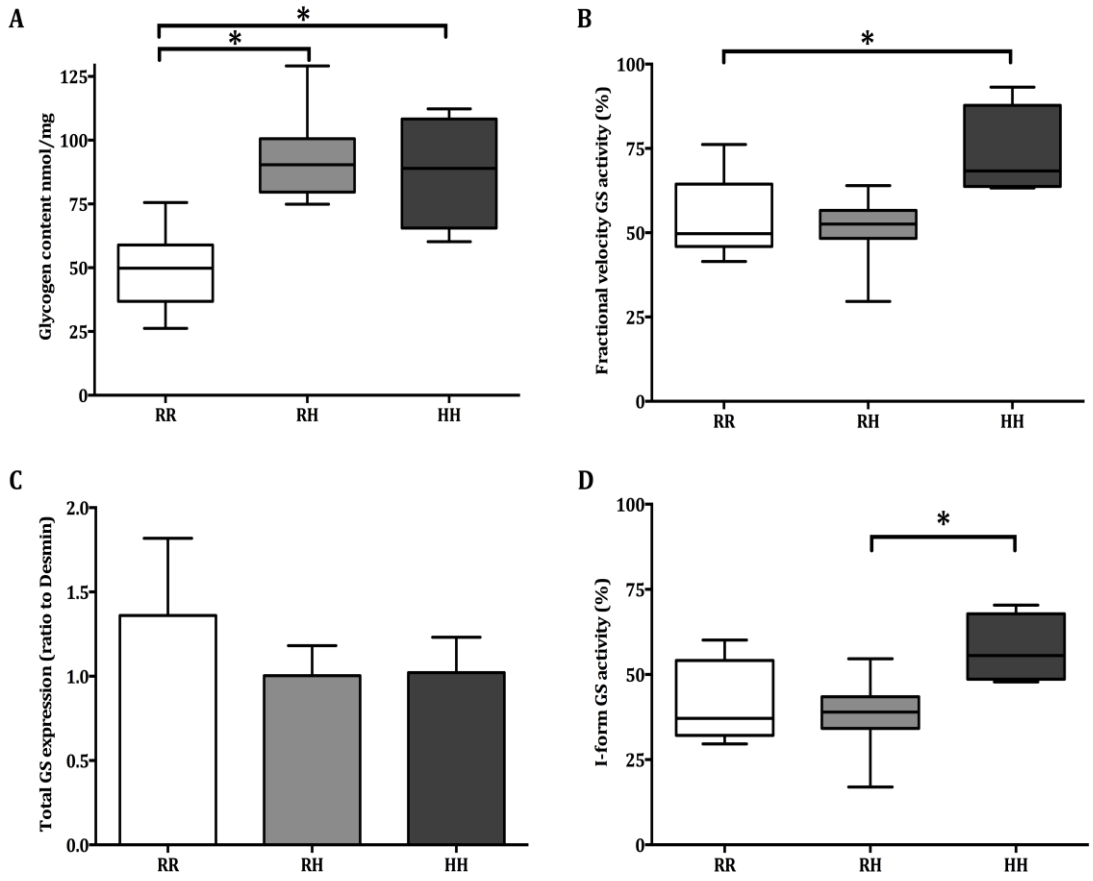

Figure 1: A) Glycogen content of wet weight muscle samples from WT (RR)(n=7), PSSM1-heterozygotes (RH)(n=8) and PSSM1-homozygotes (HH)(n=4) horses. (median +/- min/max values, box represents interquartile range; RR vs. RH p=0.005, RR vs. HH p= 0.041, *p<0.05). **B) Glycogen synthase activity shown as fractional velocity (FV) and D) I-form activity.** There was an increase in I-form activity between heterozygotes (RH) and PSSM1-homozygotes (HH) samples (p=0.04) and an increase in FV between PSSM1-homozygotes (HH) and WT controls (RR) (p=0.03) (median +/- min/max values, box represents interquartile range, RR (n= 12), RH (n=13), HH (n=4) *p<0.05**). C) Total glycogen synthase expression** in muscle homogenates showed no significant differences between the genotypes for expression of total GS (p=0.98),

Phosphorylation of GS

Mutant horse muscle samples had greater phosphorylation at site 2+2a than WT samples (Figure 2B; p=0.009), in a relationship that suggested dependency on mutant allele number. However,

there were no detectable differences in levels of phosphorylation at the other target sites (1b and 3a+b) on GS between the genotypes (Figure 2A and 2C).

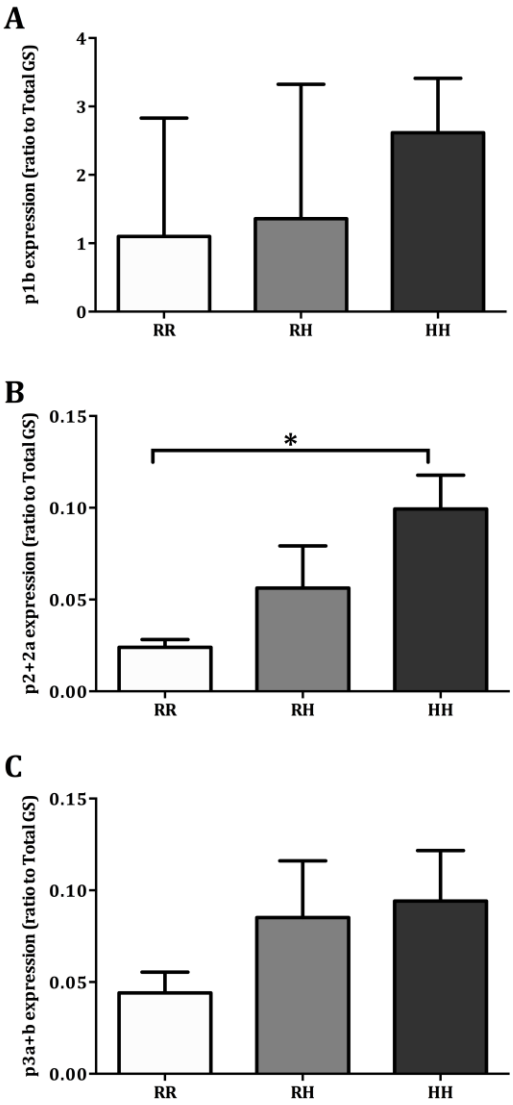

Figure 2: Western blot analysis of phosphorylated GS expression from skeletal muscle homogenates. There were no significant differences between the genotypes for expression of A) p1b isoform (p=0.48) and C) p3a+b isoform (p=0.17). There was significantly more phosphorylation at site p2+2a (B) in PSSM1-homozygotes compared to control horses (RR) (p=0.009) and there was a trend suggesting a dependence on mutant allele copy number. (Mean +/- SEM, RR (n=12) RH (n=13) HH (n=3) *p<0.05).

GLUT4, GSK3 and AMPK expression

There was no difference in GLUT4 or GSK3β protein expression between different genotypes (data not shown). However, there was significantly higher levels of AMPKα1 protein in the homozygous mutant samples compared to WT controls (Figure 3A; p=0.04) and a trend towards higher phosphorylated AMPK (pAMPK) in homozygous mutant muscle samples compared to WT and heterozygotes (Figure 3E), although this did not reach significance (p=0.13). There was a highly significant and strong association between AMPKα1 expression and pAMPK (Figure 3F; R^2=0.66, p<0.0001). There was also significantly lower AMPKβ1 expression in homozygous mutant samples compared to heterozygotes (Figure 3C; p=0.03) but not compared to WT controls.

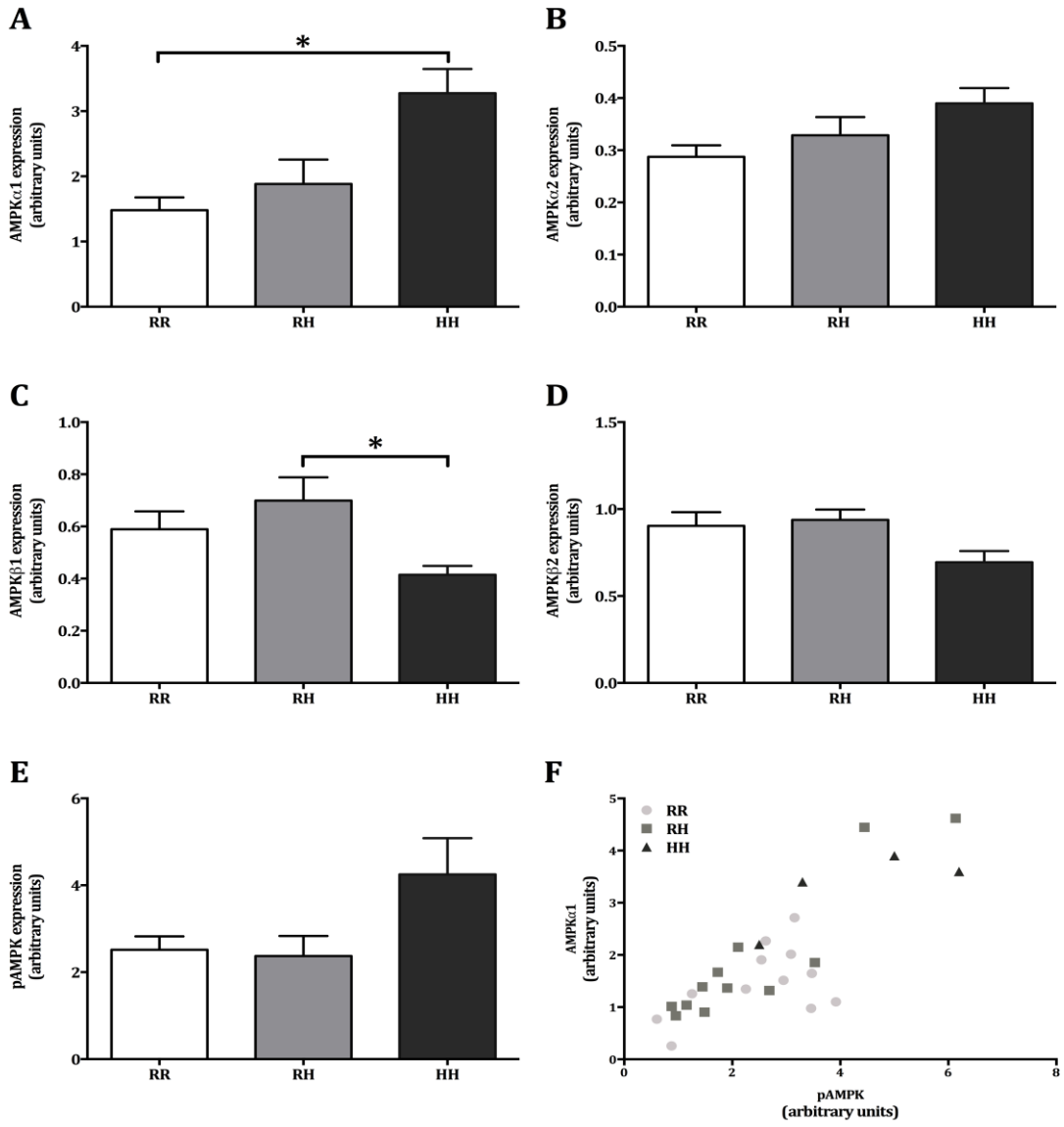

Figure 3: AMPK subunit and phosphorylation expression from skeletal muscle extracts. There were no significant differences in AMPKα2 (p=0.15) or AMPKβ2 (p=0.28) expression between different genotypes (B and D). There was a significant increase in AMPKα1 expression in homozygous mutant samples (HH) compared to heterozygotes (RH) and WT controls (RR) (A; p=0.04) and a significant decrease in AMPKβ1 expression in the homozygous mutant samples (HH) compared to the heterozygotes (C; p=0.03). There was a significant and strong correlation between AMPKα1 and pAMPK (F; R^2=0.66, p<0.0001).

GS activity is dependent on its phosphorylation; in particular phosphorylation of sites 3a, 3b and 2+2a and is highly dependent on glycogen content via negative feedback [35]. Due to the significant increase in phosphorylation at site 2+2a, correlation coefficients were calculated between site 2+2a phosphorylation and glycogen content and GS activity. Muscle glycogen content was weakly but significantly correlated with expression of the 2+2a GS isoform (R^2=0.23, p=0.04) however there was no significant association between phosphorylation at site 2+2a and GS activity (data from whole cohort; not shown).

Glycogen synthase homology modelling

The residues resolved in the G6P-bound crystal structure of yeast Gsy2p and the corresponding region of equine GS share 55% sequence identity (Figure 4). Conserved residues include the binding determinants of G6P and maltodextrin. In addition, the R309 residue of horse GS is conserved as R298 in yeast Gsy2p (Figure 4). Therefore Gsy2p structures with and without G6P bound provided suitable structural templates for homology modelling equine GS as a homotetramer with basal and active conformations, respectively (Figure 5A and 5B).

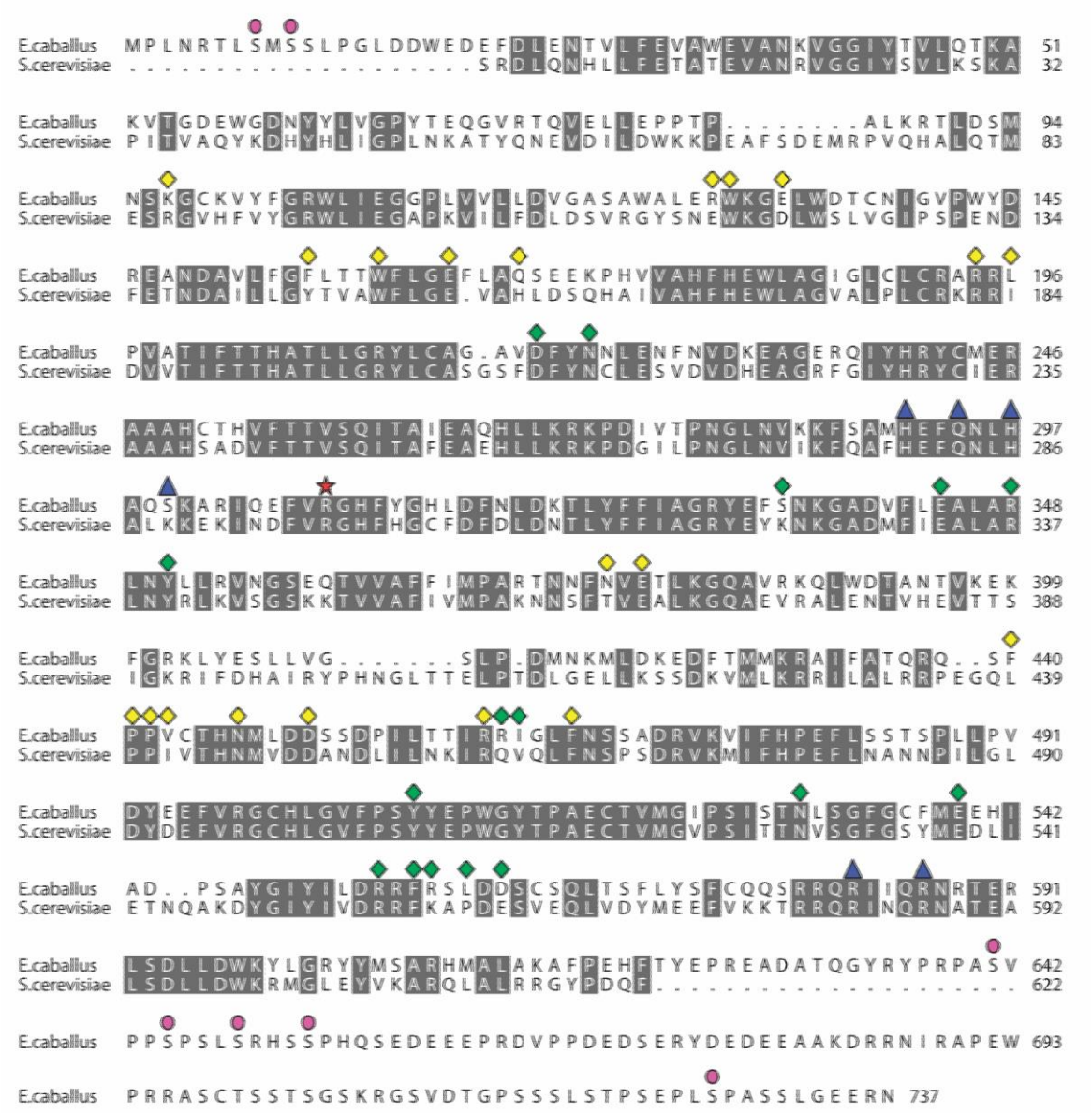

Figure 4: Sequence alignment of equine GS (Genbank accession ACB14276) and yeast Gsy2 (sequence in PDB ID 3NB0). Red star: R309 in equine GS and the location of the PSSM1-associated R309H mutation. Magenta circles: predicted phosphorylation sites. Blue triangles: binding residues of glucose-6-phosphate. Diamonds: binding residues of maltodextrin (yellow: sites 1 and 2; green: sites 3 and 4).

As a first step in understanding the structural effects of the R309H mutation, the environment around R309 was inspected in the wild-type GS models. In both basal and active GS models,

R309 is distal from the G6P and maltodextrin binding sites (Figure 5A and 5B) and is therefore not predicted to form a direct binding contact for either substrate. Nevertheless, R309 is located on the C-terminal end of an α-helix that contains four residues (H291, Q294, H297, K301) that are G6P binding determinants. In addition, R309 is positioned adjacent to a pair of α-helices that use a coiled-coil interaction to form the major interface between subunits of the tetramer. Indeed, conformational transition between basal and active states involves translation and rotation around this central tetrameric interface [26] (Figure 5A and B).

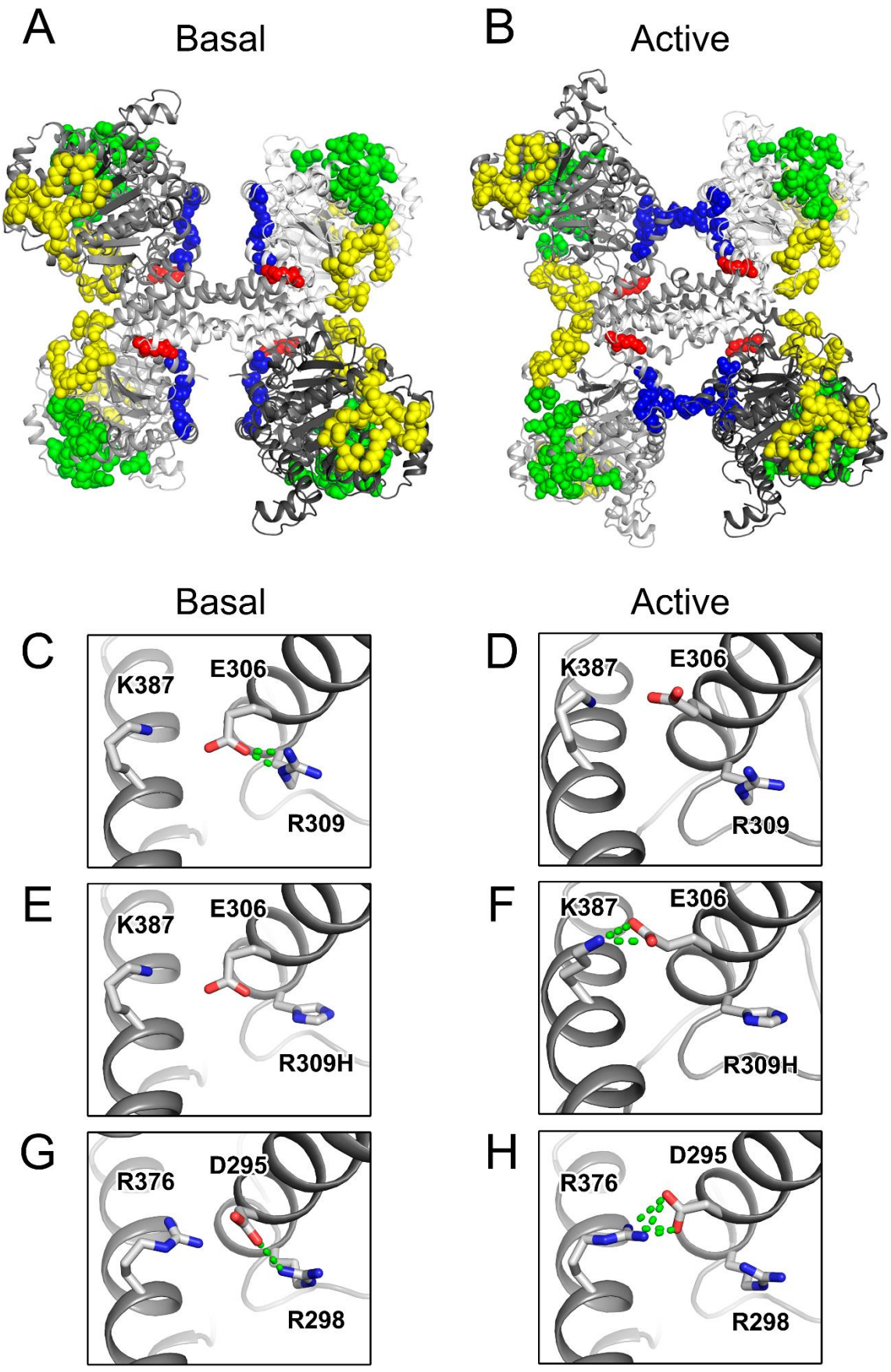
A
Basal
B
Active
Basal
Active
C
K387
E306
R309
D
K387
E306
R309
E
K387
E306
R309H
F
K387
E306
R309H
G
R376
D295
R298
H
R376
D295
R298

Figure 5: Homology models of equine GS. (A) Basal and (B) active-state equine wild-type GS model tetramers are shown as ribbons with monomers coloured different shades of grey. Residues in space-fill are R309 (red), G6P-binding contacts (blue) and maltodextrin-binding contacts (yellow: sites 1 and 2; green: sites 3 and 4). The 309 position and local charged residues are shown as sticks for WT GS [(C) basal; (D) active-state] and the PSSM1-associated R309H mutant [(E) basal; (F) active-state]. Also shown as sticks are the corresponding residues in the crystal structures of yeast Gsy2p [(G) basal; (H) active-state]. Salt bridge interactions are shown as green dashes.

R309 in the GS models and the corresponding R298 residue in the yeast Gsy2p structures make similar interactions (Figure 5C-H). Gsy2p R298 forms a salt bridge with the side chains of D295 in the basal state (Fig 5G). This interaction is lost in the active state (Figure 5H) and, whereas R298 forms no new interactions, its former interaction partner, D295, instead forms a salt bridge with residue R376. R376 is located on the adjacent α-helix that forms the aforementioned coiled-coil configuration of the enzyme subunit interface. A similar state-dependent switch in salt bridges is found with equine WT GS. R309 engages in a salt bridge with E306 and, as with Gsy2P, this interaction is lost in the active state where E306 is instead available to form a salt bridge with K387.

The R309H mutation was introduced into GS models and the predicted outcome was the elimination of the salt bridge interaction with E306 in the basal-state conformation (Figure 5E). Release of E306 from an interaction with the 309 position may instead allow it to interact with the adjacent K387 even in the basal state of the mutant enzyme.

GS kinetics

Recombinant equine GS was then used to compare WT and mutant enzyme kinetics and marked differences were detected (Table 1).

Table 1: Comparison of kinetics of WT and mutant (R309H) GS enzyme. Values given are the averages ±SEM from 3 separate experiments.

Protein	Km UDPG (-G6P)	Km UDPG (10mM G6P)	Vmax UDPG (-G6P)	Vmax UDPG (10mM G6P)	Vmax/Km (-G6P)	Vmax/Km (10mM G6P)	$S_{0.5}$ G6_ (4.4mM UDPG)
WT GS	2.4 ±0.2	1.6 ±0.1	0.05 ±0.01	3.1 ±0.1	0.023 ± 0.002	2.0 ±0.2	3.0 ±0.4
R309H GS	0.48 ±0.01	0.18 ±0.02	0.72 ±0.06	1.9 ±0.1	1.5 ±0.3	11 ±2	0.24 ±0.03

These analyses reveal that the mutant enzyme behaves as if it is nearly fully active even in the absence of its allosteric activator, G6P as is shown by the significantly lower K_m and increased V_{max} in the absence of G6P (Table 1).

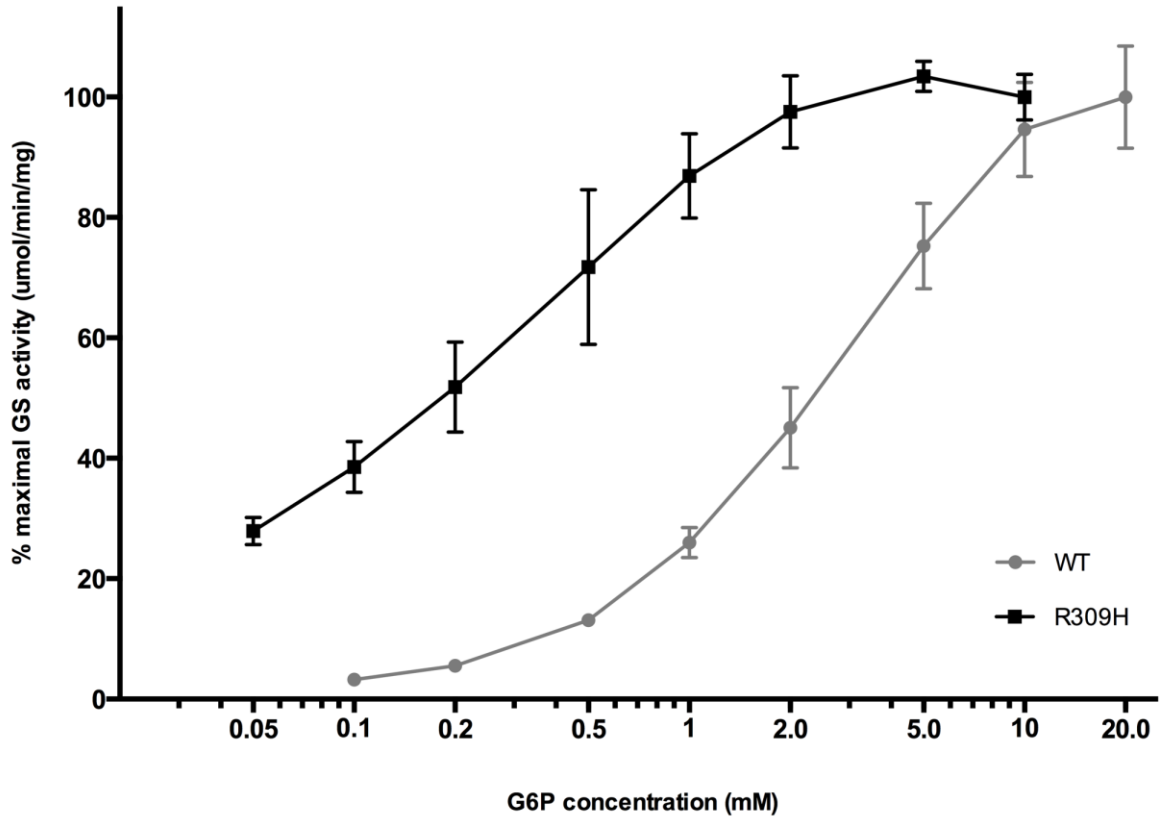

Figure 6: Glucose-6-phosphate titration curves for enzyme activity of the WT and R309H mutant enzyme. These curves show that the mutant enzyme has much higher enzyme activity at much lower concentrations of G6P and reaches its maximal activity at much lower G6P concentrations. (Mean +/- SEM on a logarithmic scale, n=3 repeats)

The G6P titration curves for the WT and the R309H mutant enzymes show that the mutant enzyme is nearing maximal activation at G6P concentrations that the WT enzyme is barely activated (Figure 6).

Table 2: Specific activity of WT and R309H mutant glycogen synthase in absence and presence of G6P (n=3).

	Specific activity –G6P (umol/min/mg)	Specific activity 10mM G6P (umol/min/mg)	Activity ratio
WT GS	0.04	2.33	0.02
R309H GS	0.68	1.63	0.41

The low activity ratio seen in the WT enzyme is similar to that seen in baculovirus generated human GS [48] and the R309H mutant enzyme shows an approximately 20 fold higher activity ratio (Table 2), due largely to the marked activation that occurs in the mutant enzyme, in the absence of G6P.

Discussion

PSSM1, caused by a missense mutation in the equine *GYS1* gene [8] is histopathologically characterised by increased amylopectate and glycogen in skeletal muscle fibres [49]. Here, we investigated the protein structure, glycogen content, GS expression, regulation and activity in skeletal muscle samples and in mutant and wild type recombinant enzymes, in order to determine whether the increased GS activity in PSSM1-affected muscle, reported by McCue *et al*. [8] was associated with altered enzyme expression, altered upstream regulation or a conformational change with possible constitutive activation. Our results reveal that the R309H founder mutation, responsible for this highly prevalent equine myopathy, present in over 20 breeds worldwide, is caused by constitutive activation; furthermore, we propose a feasible structural mechanism based on our modelling analyses.

Similar to previous results in another affected breed, we have shown that mutant draught horses have increased muscle glycogen storage [50] despite normal GLUT4 transporter expression [50]. There was no difference in total GS expression between controls and PSSM1-affected horses,

but PSSM1-affected homozygotes had increased GS activity. GS in skeletal muscle from homozygous mutant horses had increased G6P-independent activity, consistent with data from McCue *et al.,* who detected higher GS activity, irrespective of G6P concentration, in PSSM1-affected Quarter Horses [8]. As GS activity is inversely correlated to the extent of site 2+2a GS phosphorylation in normal muscle [35, 38, 51], the higher enzyme activity in mutant horses cannot be explained by inappropriate (i.e. reduced) GS phosphorylation in mutant animals, since affected horses showed significantly more GS phosphorylation at sites 2+2a, (and no difference in phosphorylation at other sites). However, as would be expected in normal muscle [36], PSSM1-affected horses had increased phosphorylation at site 2+2a, in the presence of elevated muscle glycogen, most likely reflecting a normal physiological attempt to reduce enzyme activity [35, 51-53]; indeed, the high GS activity in mutant horses occurs despite the phosphorylation and increased expression of the principal upstream kinase for phosphorylation at site 2+2a (AMPK). This lack of correlation suggests that the mutant enzyme is not regulated by lowered activity when phosphorylated at site 2+2a.

It is notable that in our study, certain effects were only detectable in PSSM1-homozygotes compared with controls, rather than between heterozygotes and controls. This might relate to an exaggerated (compensatory) effect of protein derived from the normal allele in heterozygotes or might simply reflect a more modest phenotype that was not detectable in the number of samples analysed. In contrast, McCue *et al.* reported differences between PSSM1-heterozygotes and WT controls [8]; which might relate to the higher proportion of glycolytic fibres seen in their Quarter Horses compared with our draught horses: glycogen accumulation tends to be most prominent in glycolytic fibres [54].

The phosphorylation sites of muscle GS are located on the N- and C- termini of the enzyme [55, 56]. We were unable to use homology modelling to investigate these sites as there are no corresponding regions resolved in the yeast Gsy2p structures. Nevertheless, the region around R309 was modelled (Figure 5) and, although not predicted to form a binding contact for G6P or maltodextrin (Figure 5A and 5B), this residue is positioned at a pivotal position near the tetrameric

interface of the enzyme and is located on an α-helix that harbours 4 G6P binding residues. Therefore, a structural perturbation at the 309 position could influence the position of the conformational equilibrium making it easier to adopt the active conformation. Modelling indicates that in the enzyme's basal state, R309 engages in a salt bridge with E306 whereas in the active state E306 forms an alternative salt bridge with K387 (Figure 5C and D). These salt bridge interactions might be important for stabilising the conformation of their respective functional states. We therefore propose that the effect of the R309H mutation, which is predicted to eliminate the basal-state salt bridge (Figure 5E), likely shifts the conformational equilibrium of the enzyme to the active state and reduces its tendency to adopt an inhibited state (Figure 5F). Interestingly, the residue adjacent to R309 is conserved as a glycine in both equine GS (G310) and yeast Gsy2p (G299) and its mutation results in increased Gsy2p activity [17]. This glycine is located at a turn at the C-terminal end of the helix containing R298 (equivalent to equine R309) and G6P binding contacts. It is therefore positioned to function as a typical glycine-hinge residue and the reported mutation-associated change in enzyme activity [15], provides further evidence that structural deviations in this region can produce constitutive activation.

Taken together, the increased activity detectable in horse muscle, seems most likely to be a constitutive change in the mutant enzyme's function, similar to that of the yeast mutant that also fails to respond appropriately to phosphorylation [8, 17] and also fails to respond as expected to increased glycogen content [57]. In order to test this hypothesis, enzyme kinetic studies were performed using purified recombinant protein. These studies confirmed that the mutant enzyme was almost fully active at low G6P concentrations (Table 1): i.e. it is constitutively active. The activity ratio of the WT equine enzyme was similar to that seen of human GS purified in a similar manner; further, there was no detectable difference in the extent of phosphorylation between the WT and mutant recombinant enzymes (data not shown) that could explain these significant differences in enzyme kinetics. Our data therefore confirms that the R309H mutation associated with PSSM1 is a true gain of function mutation.

In summary, our work provides further evidence that support findings of a previous study [8] that revealed that that PSSM1-associated R309H *GYS1* mutation results in increased glycogen content and GS activity in skeletal muscle. We now show that this elevated activity occurs despite hyperphosphorylation at site 2+2a and increased expression of AMPK, and for the first time, we suggest through predictive modelling a potential mechanism by which this occurs□□ Additional work is needed to explain all the phenotypic features of this equine disorder, including the intermittent rhabdomyolysis seen in some affected horses. However, our results suggest that therapeutic modification of AMPK activity, might be ineffective in mutant animals, as increased GS phosphorylation does not reduce the mutant enzyme's hyperactivity; instead, efforts aimed at direct enzyme inhibition might be more effective. Finally, dysregulation of GS or other related enzymes should be considered in humans and other animals with glycogen storage diseases of unknown origin, particularly when a dominant mode of inheritance is identified; indeed, this common equine disease represents a large animal model for evaluation of treatments aimed at reducing polyglucosan formation in skeletal muscle [33], a feature of a number of important, but comparatively rare, human myopathic disorders.

Acknowledgements

We thank the staff at Auburn University for providing the muscle samples for this work and Professor Bonnie Wallace at Birkbeck University for her advice on homology modelling. This work was partly funded by The Petplan Charitable Trust and by the Morris Animal Foundation.

References

1. Wilson, W.A., et al., *Regulation of glycogen metabolism in yeast and bacteria.* FEMS Microbiol Rev, 2010. **34**(6): p. 952-85.
2. Buschiazzo, A., et al., *Crystal structure of glycogen synthase: homologous enzymes catalyze glycogen synthesis and degradation.* Embo J, 2004. **23**(16): p. 3196-205.
3. Jensen, J. and Y.C. Lai, *Regulation of muscle glycogen synthase phosphorylation and kinetic properties by insulin, exercise, adrenaline and role in insulin resistance.* Arch Physiol Biochem, 2009. **115**(1): p. 13-21.
4. Gregory, B.L., et al., *Glycogen storage disease type IIIa in curly-coated retrievers.* J Vet Intern Med, 2007. **21**(1): p. 40-6.
5. Lohi, H., et al., *Expanded repeat in canine epilepsy.* Science, 2005. **307**(5706): p. 81.
6. Ozen, H., *Glycogen storage diseases: new perspectives.* World J Gastroenterol, 2007. **13**(18): p. 2541-53.
7. Fyfe, J.C., et al., *Glycogen storage disease type IV: inherited deficiency of branching enzyme activity in cats.* Pediatr Res, 1992. **32**(6): p. 719-25.
8. McCue, M.E., et al., *Glycogen synthase (GYS1) mutation causes a novel skeletal muscle glycogenosis.* Genomics, 2008. **91**(5): p. 458-66.
9. Naylor, R.J., et al., *Evaluation of cardiac phenotype in horses with type 1 polysaccharide storage myopathy.* J Vet Intern Med, 2012. **26**(6): p. 1464-9.
10. Stanley, R.L., et al., *A glycogen synthase 1 mutation associated with equine polysaccharide storage myopathy and exertional rhabdomyolysis occurs in a variety of UK breeds.* Equine Vet J, 2009. **41**(6): p. 597-601.
11. Herszberg, B., et al., *A GYS1 gene mutation is highly associated with polysaccharide storage myopathy in Cob Normand draught horses.* Anim Genet, 2009. **40**(1): p. 94-6.
12. Schwarz, B., et al., *Estimated prevalence of the GYS-1 mutation in healthy Austrian Haflingers.* Vet Rec, 2011. **169**(22): p. 583.
13. Johlig, L., et al., *Epidemiological and genetic study of exertional rhabdomyolysis in a Warmblood horse family in Switzerland.* Equine Vet J, 2011. **43**(2): p. 240-5.
14. McCoy, A.M., et al., *Evidence of positive selection for a glycogen synthase (GYS1) mutation in domestic horse populations.* J Hered, 2014. **105**(2): p. 163-72.
15. Pederson, B.A., et al., *Overexpression of glycogen synthase in mouse muscle results in less branched glycogen.* Biochem Biophys Res Commun, 2003. **305**(4): p. 826-30.
16. Valberg, S.J., et al., *Glycogen branching enzyme deficiency in quarter horse foals.* J Vet Intern Med, 2001. **15**(6): p. 572-80.
17. Anderson, C. and K. Tatchell, *Hyperactive glycogen synthase mutants of Saccharomyces cerevisiae suppress the glc7-1 protein phosphatase mutant.* J Bacteriol, 2001. **183**(3): p. 821-9.
18. Prats, C., et al., *Phosphorylation-dependent translocation of glycogen synthase to a novel structure during glycogen resynthesis.* J Biol Chem, 2005. **280**(24): p. 23165-72.
19. Roach, P.J., *Glycogen and its metabolism.* Curr Mol Med, 2002. **2**(2): p. 101-20.
20. Skurat, A.V., Y. Wang, and P.J. Roach, *Rabbit skeletal muscle glycogen synthase expressed in COS cells. Identification of regulatory phosphorylation sites.* J Biol Chem, 1994. **269**(41): p. 25534-42.
21. Roach, P.J., *Control of glycogen synthase by hierarchal protein phosphorylation.* FASEB J, 1990. **4**(12): p. 2961-8.
22. Bouskila, M., et al., *Allosteric regulation of glycogen synthase controls glycogen synthesis in muscle.* Cell Metab, 2010. **12**(5): p. 456-66.
23. Witczak, C.A., C.G. Sharoff, and L.J. Goodyear, *AMP-activated protein kinase in skeletal muscle: from structure and localization to its role as a master regulator of cellular metabolism.* Cell Mol Life Sci, 2008. **65**(23): p. 3737-55.

24. Wojtaszewski, J.F., et al., *Isoform-specific and exercise intensity-dependent activation of 5'-AMP-activated protein kinase in human skeletal muscle.* J Physiol, 2000. **528 Pt 1**: p. 221-6.
25. Dranchak, P.K., et al., *Biochemical and genetic evaluation of the role of AMP-activated protein kinase in polysaccharide storage myopathy in Quarter Horses.* Am J Vet Res, 2007. **68**(10): p. 1079-84.
26. Baskaran, S., et al., *Structural basis for glucose-6-phosphate activation of glycogen synthase.* Proc Natl Acad Sci U S A, 2010. **107**(41): p. 17563-8.
27. Zeqiraj, E., et al., *Structural basis for the recruitment of glycogen synthase by glycogenin.* Proc Natl Acad Sci U S A, 2014. **111**(28): p. E2831-40.
28. Landau, M., et al., *ConSurf 2005: the projection of evolutionary conservation scores of residues on protein structures.* Nucleic Acids Res, 2005. **33**(Web Server issue): p. W299-302.
29. Pederson, B.A., et al., *Regulation of glycogen synthase. Identification of residues involved in regulation by the allosteric ligand glucose-6-P and by phosphorylation.* J Biol Chem, 2000. **275**(36): p. 27753-61.
30. Furukawa, K., et al., *Identification of Lys277 at the active site of Escherichia coli glycogen synthase. Application of affinity labeling combined with site-directed mutagenesis.* J Biol Chem, 1994. **269**(2): p. 868-71.
31. Baskaran, S., et al., *Multiple glycogen-binding sites in eukaryotic glycogen synthase are required for high catalytic efficiency toward glycogen.* J Biol Chem, 2011. **286**(39): p. 33999-4006.
32. Suzuki, Y., et al., *Insulin control of glycogen metabolism in knockout mice lacking the muscle-specific protein phosphatase PP1G/RGL.* Mol Cell Biol, 2001. **21**(8): p. 2683-94.
33. Hedberg-Oldfors, C. and A. Oldfors, *Polyglucosan storage myopathies.* Mol Aspects Med, 2015. **46**: p. 85-100.
34. Chan, T.M. and J.H. Exton, *A rapid method for the determination of glycogen content and radioactivity in small quantities of tissue or isolated hepatocytes.* Anal Biochem, 1976. **71**(1): p. 96-105.
35. Prats, C., et al., *Dual regulation of muscle glycogen synthase during exercise by activation and compartmentalization.* J Biol Chem, 2009. **284**(23): p. 15692-700.
36. Jensen, J., et al., *Muscle glycogen inharmoniously regulates glycogen synthase activity, glucose uptake, and proximal insulin signaling.* Am J Physiol Endocrinol Metab, 2006. **290**(1): p. E154-E162.
37. Jensen, J., et al., *Improved insulin-stimulated glucose uptake and glycogen synthase activation in rat skeletal muscles after adrenaline infusion: role of glycogen content and PKB phosphorylation.* Acta Physiol Scand, 2005. **184**(2): p. 121-30.
38. Hojlund, K., et al., *Increased phosphorylation of skeletal muscle glycogen synthase at NH2-terminal sites during physiological hyperinsulinemia in type 2 diabetes.* Diabetes, 2003. **52**(6): p. 1393-402.
39. Woods, A., et al., *The alpha1 and alpha2 isoforms of the AMP-activated protein kinase have similar activities in rat liver but exhibit differences in substrate specificity in vitro.* FEBS Lett, 1996. **397**(2-3): p. 347-51.
40. Durante, P.E., et al., *Effects of endurance training on activity and expression of AMP-activated protein kinase isoforms in rat muscles.* Am J Physiol Endocrinol Metab, 2002. **283**(1): p. E178-86.
41. Højlund, K., et al., *AMPK activity and isoform protein expression are similar in muscle of obese subjects with and without type 2 diabetes.* Am J Physiol Endocrinol Metab, 2004. **286**(2): p. E239-44.
42. Sievers, F., et al., *Fast, scalable generation of high-quality protein multiple sequence alignments using Clustal Omega.* Mol Syst Biol, 2011. **7**: p. 539.
43. Eswar, N., et al., *Comparative protein structure modeling using MODELLER.* Curr Protoc Protein Sci, 2007. **Chapter 2**: p. Unit 2.9.

44. Willard, L., et al., *VADAR: a web server for quantitative evaluation of protein structure quality.* Nucleic Acids Res, 2003. **31**(13): p. 3316-9.
45. Guex, N., A. Diemand, and M.C. Peitsch, *Protein modelling for all.* Trends Biochem Sci, 1999. **24**(9): p. 364-7.
46. Zhang, W., A.A. DePaoli-Roach, and P.J. Roach, *Mechanisms of multisite phosphorylation and inactivation of rabbit muscle glycogen synthase.* Arch Biochem Biophys, 1993. **304**(1): p. 219-25.
47. Thomas, J.A., K.K. Schlender, and J. Larner, *A rapid filter paper assay for UDPglucose-glycogen glucosyltransferase, including an improved biosynthesis of UDP-14C-glucose.* Anal Biochem, 1968. **25**(1): p. 486-99.
48. Khanna, M., et al., *Expression and purification of functional human glycogen synthase-1 (hGYS1) in insect cells.* Protein Expr Purif, 2013. **90**(2): p. 78-83.
49. McCue, M.E., W.P. Ribeiro, and S.J. Valberg, *Prevalence of polysaccharide storage myopathy in horses with neuromuscular disorders.* Equine Vet J Suppl, 2006(36): p. 340-4.
50. Annandale, E.J., et al., *Insulin sensitivity and skeletal muscle glucose transport in horses with equine polysaccharide storage myopathy.* Neuromuscul Disord, 2004. **14**(10): p. 666-74.
51. Hojlund, K., et al., *Dysregulation of glycogen synthase COOH- and NH2-terminal phosphorylation by insulin in obesity and type 2 diabetes mellitus.* J Clin Endocrinol Metab, 2009. **94**(11): p. 4547-56.
52. Jorgensen, S.B., et al., *The alpha2-5'AMP-activated protein kinase is a site 2 glycogen synthase kinase in skeletal muscle and is responsive to glucose loading.* Diabetes, 2004. **53**(12): p. 3074-81.
53. Wojtaszewski, J.F., et al., *Glycogen-dependent effects of 5-aminoimidazole-4-carboxamide (AICA)-riboside on AMP-activated protein kinase and glycogen synthase activities in rat skeletal muscle.* Diabetes, 2002. **51**(2): p. 284-92.
54. Naylor, R.J., et al., *Allele copy number and underlying pathology are associated with subclinical severity in equine type 1 polysaccharide storage myopathy (PSSM1).* PLoS One, 2012. **7**(7): p. e42317.
55. Ros, S., et al., *Control of liver glycogen synthase activity and intracellular distribution by phosphorylation.* J Biol Chem, 2009. **284**(10): p. 6370-8.
56. Nielsen, J.N. and J.F. Wojtaszewski, *Regulation of glycogen synthase activity and phosphorylation by exercise.* Proc Nutr Soc, 2004. **63**(2): p. 233-7.
57. Lai, Y.C., et al., *Glycogen content and contraction regulate glycogen synthase phosphorylation and affinity for UDP-glucose in rat skeletal muscles.* Am J Physiol Endocrinol Metab, 2007. **293**(6): p. E1622-9.

Supplementary data

Table S 1: Breed and signalment data for horses used in this study.

	RR (n=12)	***RH (n=13)***	***HH (n=4)***
Age *(mean+/- SD)*	10 (3.3)	9.7 (3.1)	9.3 (3.4)
Sex			
Male	6	6	2
Female	6	7	2
Breed			
Belgian	5	7	2
Percheron	7	6	2

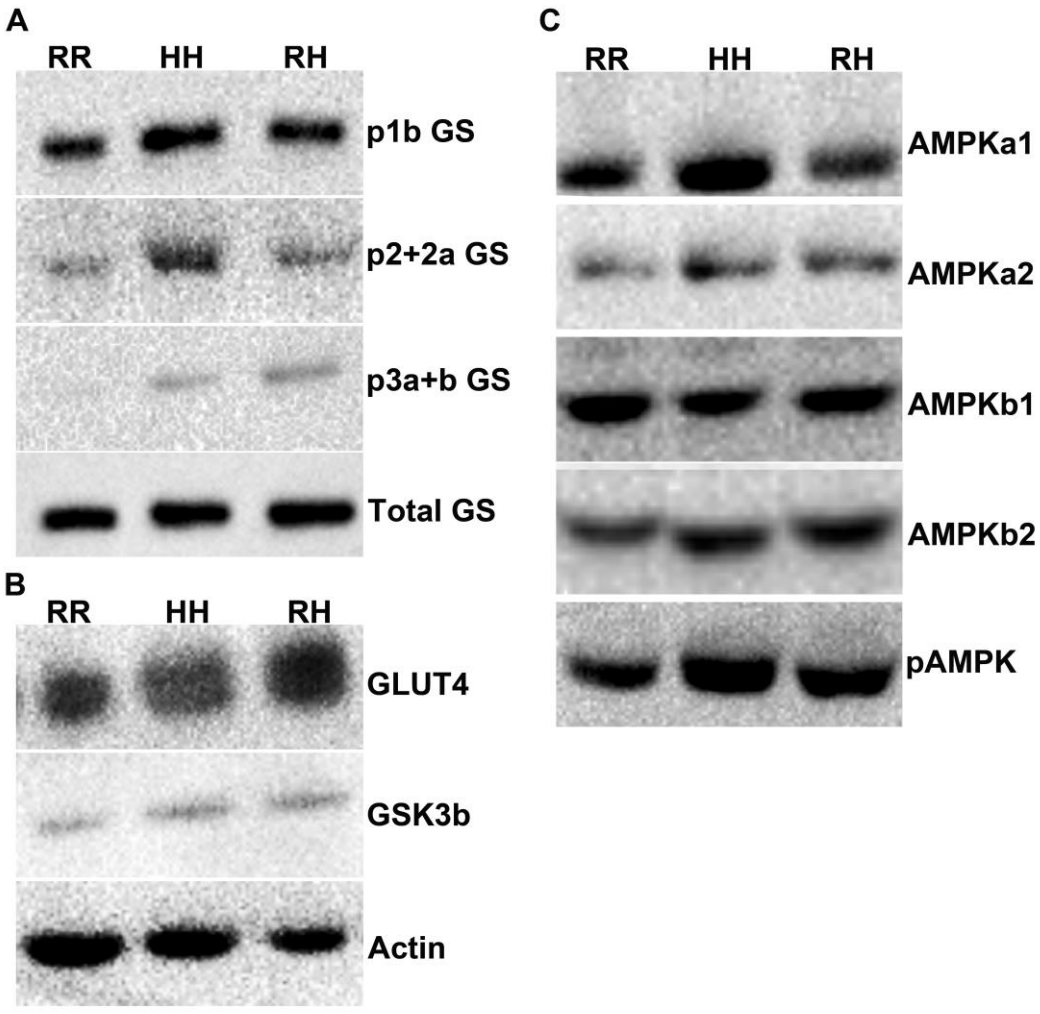

Figure S1: Example western blots. A) Glycogen synthase antibodies, B) upstream kinases and actin and C) AMPK antibodies as optimised for use in equine muscle lysates.

Declaration of funding and conflict of interest

Parts of this study were funded by grants from Petplan Charitable Trust and the Morris Animal Foundation.